Journal of Organometallic Chemistry, 272 (1984) 207–229
Elsevier Sequoia S.A., Lausanne – Printed in The Netherlands

SYNTHESIS OF HYDRIDOTRIOSMIUM COMPLEXES CONTAINING ISOMERIC μ-CARBOXAMIDO, $\{\mu(O, C)$–O=C(NHR)$\}$, μ-FORMAMIDO, $\{\mu(O, N)$–O=C(H)N(R)$\}$, AND μ-IMINYL, $\{\mu(C, N)$–C(OR′)=NR$\}$, GROUPS. CRYSTAL AND MOLECULAR STRUCTURE OF $Os_3\{\mu$-H,μ-C(OR′)=NCH$_3\}$-$(CO)_{10}$, R′ = C(=O)NHCH$_3$ *

YING-CHIH LIN **, ANDREAS MAYR, CAROLYN B. KNOBLER and HERBERT D. KAESZ *
Department of Chemistry and Biochemistry, University of California, Los Angeles, California, 90024 (U.S.A.)

(Received February 28th, 1984)

Summary

Primary or secondary aliphatic amines are observed to react with $Os_3(CO)_{12}$ in excess amine or other polar solvents at temperatures in the range −10 to 25 °C. One mole of CO is evolved and a $\mu(O,C)$-carboxamido complex (**1**) is isolated in high yield: $Os_3\{\mu$-H,μ-O=CNR′R$\}(CO)_{10}$ (**1a**, R = Me, R′ = H; **1b**, R = R′ = Me; **1c**, R = n-Pr, R′ = H, **1d**, R = n-Bu, R′ = H; **1e**, R = Et, R′ = H). The ^{1}H NMR spectrum of **1e** indicates the existence of two isomers due to the restricted rotation around the C–N bond of the μ-carboxamido group.

Reaction of methyl or ethyl isocyanate with $Os_3\{\mu$-H$\}_2(CO)_{10}$ at room temperature under N_2 gives three principal products: a $\mu(O,N)$-formamido complex, $Os_3\{\mu$-H,μ-OC(H)NR$\}(CO)_{10}$ (**2**), the $\mu(O,C)$-carboxamido complex, **1**, and a $\mu(C,N)$-iminylurethane complex, $Os_3\{\mu$-H,μ-C(OR′)=NR$\}(CO)_{10}$, (**4**, R′ = C(=O)NHR). Product **1** in this reaction arises from isomerization of an intermediate $\mu(C,N)$-hydroxyiminyl complex, $Os_3\{\mu$-H,μ-C(OH)=NR$\}(CO)_{10}$ (**3**). This complex is isolated upon initial chromatography of the reaction mixture. For the isomerization of **3** to **1**, $t_{1/2}$ 17.5 d in $CDCl_3$ solution, E_a 92 kJ/mol. Spectroscopic data indicate that **3** is a mixture of tautomers in ratio of 19/1 in $CDCl_3$: $Os_3\{\mu$-H,μ-C(OH)=NCH$_3\}(CO)_{10}$ (**3**-enol) and $Os_3\{\mu$-H,μ-C(=O)N(H)CH$_3\}(CO)_{10}$ (**3**-keto).

The structure of **4** has been determined at −158 °C using a Syntex $P\bar{1}$ computer-automated diffractometer and graphite-monochromatized Mo-K_α radiation. Some 2936 unique reflections with $I > 3\sigma(I)$ were used in the refinement to give final discrepancy indices of $R = 0.030$ and $R_w = 0.037$. The complex crystallizes in the monoclinic space group $P2_1/c$ in a cell having the dimensions of a 13.413(3) Å, b 16.712(3) Å, c 9.400(3) Å, and β 95.01(2)°. The calculated density is 3.06 g cm^{-3}.

* Dedicated to Professor Sei Otsuka.
** Taken in part from the Dissertation of Y.C. Lin [3a].

0022-328X/84/$03.00

The location of the three Os atoms was determined from the Patterson map. All other nonhydrogen atoms were then located by difference maps. The two hydrogen atoms, one bridging the edge of the cluster and the other attached to the nitrogen atom, were located after all but the two methyl carbon atoms were refined anisotropically; the latter two atoms were included in the refinement as members of rigid methyl groups. The crystal consists of discrete molecules. Three osmium atoms form a nearly isosceles triangle (Os(1)–Os(2) 2.882(1) Å, Os(1)–Os(3) 2.881(1) Å, Os(2)–Os(3) 2.923(1) Å). An *N*-methyl-iminyl group with a urethane derivative on the carbon atom is bridging across Os(2) and Os(3) through the carbon and nitrogen atoms, respectively. The two metal atoms Os(2) and Os(3) are also bridged by a hydrogen atom outside the trimetal plane and away from the bridging iminyl group. The metal bonded carbonyl groups are all terminal.

Introduction

Earlier observations of the stepwise reduction of acetonitrile on the face of a triiron cluster complex [1] prompted us to investigate the reactions of primary or secondary alkyl amines with $Ru_3(CO)_{12}$ and $Os_3(CO)_{12}$ to see if we could enter a similar cycle for these heavier congeners of iron. We observed instead formation of edge double-bridged {μ-H,μ-carboxamido} derivatives as we reported for $Ru_3(CO)_{12}$ [2]. The present paper describes our results for $Os_3(CO)_{12}$ and the synthesis of isomeric complexes through reaction of $Os_3\{\mu\text{-H}\}_2(CO)_{10}$ with methyl isocyanate; portions of this work have been reported in preliminary form [3].

Carboxamido complexes have been obtained in the reaction of $PhCH_2NH_2$ with $Os_3(CO)_{12}$ in refluxing octane [4]; these are produced in low yield and are accompanied by the edge-bridged amido complex $Os_3\{\mu\text{-H},\mu\text{-NHCH}_2\text{Ph}\}(CO)_{10}$ among other products. Other carboxamido complexes have been obtained in the reaction of a variety of amides [5a] or *N*,*N*-dimethyl formamide [5b] with $Os_3(CO)_{10}(CH_3CN)_2$ in refluxing cyclohexane or refluxing THF; yields are in the range 35–70%. None of these routes compare favorably with that reported here. Finally, a parallel and independent study was reported for the reaction of aryl isocyanates with $Os_3\{\mu\text{-H}\}_2(CO)_{10}$ [6]; a $\mu(O,N)$-formamido complex is observed as the principal product with only minor amounts of the carboxamido complex; further reference to this work is made in the discussion section below.

Results

Synthesis of $\mu(O,C)$-bonded carboxamido complexes

The reaction of $Os_3(CO)_{12}$ with neat alkyl amine is summarized in eq. 1 *. The structure of the product as a $\mu(O,C)$-carboxamido complex is deduced by spectral similarities with that of the homologous triruthenium complex $Ru_3[\mu\text{-H},\mu\text{-O=CNMe}_2\}(CO)_{10}$ whose structure was determined by X-ray diffraction [2].

* The conventional vector between metal atoms of the double-bridged edge is omitted from our structure representations of trinuclear cluster complexes because we believe this better reflects the octahedral coordination around the metal atoms in question. Bonding interactions between metal atoms of a double-bridged edge are believed to take place through orbitals involving the bridging atoms, see [7].

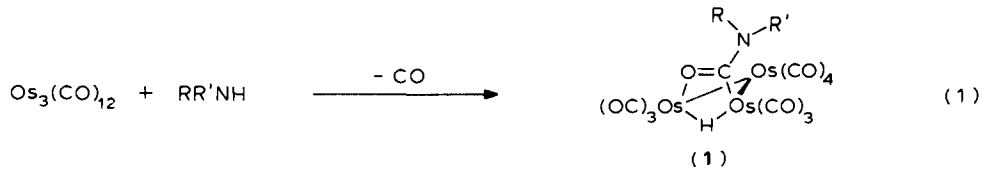

(1)

(**1a**, R = Me, R' = H, **1b**, R = R' = Me, **1c**, R = n-Pr, R' = H; **1d**, R = n-Bu, R' = H, **1e**, R = Et, R' = H)

$O{=}CNMe_2\}(CO)_{10}$ whose structure was determined by X-ray diffraction [2].

The reaction of $Os_3(CO)_{12}$ with propylamine occurs at room temperature under nitrogen; the solution first turns to deep orange within about 15 min. If the amine is removed at this stage $Os_3(CO)_{12}$ can be recovered quantitatively. If the reaction is allowed to continue, CO loss takes place even under these mild conditions. The reaction proceeds to completion overnight. The carboxamido complex $Os_3\{\mu\text{-}H,\mu\text{-}O{=}CN(H)\text{-}n\text{-}Pr\}(CO)_{10}$ (**1c**) is isolated in high yield. Purification is accomplished by column chromatography followed by recrystallization from either hexane or hexane-dichloromethane solution at low temperature. Spectroscopic data for **1** are listed in Tables 1 and 2. An oily product is obtained in very low quantity, suspected to be $H_2Os_3(O{=}CNRR')_2(CO)_8$, by comparison of its IR spectrum with that of $H_2Os_3(PhC{=}NMe)_2(CO)_8$ [8]. Owing to its low yield, purification was difficult and no further characterization was carried out.

Analogous carboxamido complexes **1a**, **1b** and **1e** are obtained utilizing the neat amine in the same experimental procedure, see eq. 1; temperatures must be between −10 and 6 °C to keep the neat amines in the liquid form. The reaction times are thus unavoidably long, up to two days, due to the lower temperatures.

Spectroscopic features of μ(O,C)-bonded carboxamido complexes, (1)

The mass spectrum of the methyl complex, **1a**, indicates a parent molecular ion

TABLE 1

IR DATA [a]

	ν(CO)
1a	2108(w), 2067(s), 2056(s), 2023(s), 2011(s), 1993(m), 1985(w,sh), 1977(w)
	3459(ν(N–H)), 2956(ν(Me)), 1475(δ(Me))
2a	2109(m), 2070(s) 2059(s), 2025(vs), 2013(s), 2012(s,sh), 2000(m), 1989(w), 1988(w,sh), 1980(w)
	2912(ν(Me)), 1601(ν(O–CH=N)), 1450(δ(Me))
3a	2107(m), 2065(vs), 2055(s), 2024(s), 2013(s), 2006(m), 1992(s), 1977(w)
	3595(ν(OH)), 3314(ν(OH..O)), 2926(ν(Me)), 1793(ν(C=O)), 1618(ν(C=N))
4a	2107(m), 2068(vs), 2056(s), 2025(vs), 2010(m,sh), 2003(m), 1995(m), 1979(w)
	3464(ν(NH)), 2926(ν(Me)), 1776(ν(C=O)), 1593(ν(C=N)), 1503(δ(Me),δ(NH)), 1221(ν(C-O))

[a] Complexes with different alkyl groups have essentially the same IR spectra in the carbonyl stretching region. For the terminal ν(CO) stretching, the spectra were obtained in hexane. Full range spectra in $CCl_2{=}CCl_2$.

TABLE 2

^{1}H NMR DATA [a]

1a	5.86(br, NH), 2.63(d, CH_3, J(H–H) 4.4 Hz), −14.25(s, Os–H–Os)
1b	3.09(s, CH_3), 2.75(s, CH_3), −13.87(s, Os–H–Os)
1e	5.79(br, NH), 3.16(m, two $ABXY_3$s, CH_2), 1.05(t, CH_3, J(H–H) 7.7 Hz), −14.27(s, Os–H–Os)
1c	5.80(br, NH), 3.07(m, CH_2), 1.41(m, CH_2), 0.84(t, CH_3, J(H–H) 7.7 Hz), −14.28(s, Os–H–Os)
1d	5.77(br, NH), 3.11(m, CH_2), 1.33(m, two CH_2), 0.88(t, J(H–H) 7.7 Hz) −14.29(s, Os–H–Os)
2a	7.51(s, C*H*), 3.27(s, CH_3), −11.46(s, Os–H–Os)
2b	7.57(s, C*H*), 3.50(m, CH_2), 1.14(t, CH_3, J(H–H) 7.0 Hz), −11.44(s, Os–H–Os)
3a	6.79(br, OH), 3.05(s, CH_3), −15.45(s, Os–H–Os)
3b	6.35(br, O*H*), 3.37(m, ABX_3, CH_2), 0.98(t, CH_3, J(H–H) 7.1 Hz), −15.47(s, Os–H–Os)
4a	4.94(br, NH), 3.11(s, CH_3), 2.86(d, CH_3, J(H–H) 5.6 Hz), −15.20(s, Os–H–Os)
4b	4.94(br, N*H*), 3.41(m, AXY_3, CH_2), 3.28(m, ABX_3, CH_2), 1.20(t, CH_3, J(H–H) 7.3 Hz), 1.00(t, CH_3, J(H–H) 7.1 Hz), −15.23(s, Os–H–Os)

[a] $CDCl_3$ solution.

multiplet whose principal peak is measured at $m/e = 915$ (^{192}Os); this is accompanied by multiplets of fragments corresponding to successive loss of ten CO groups. One can also see faint traces of a CO-loss series of a fragment somewhat below the parent ion. This was not identified. Additionally, a CO-loss series corresponding to doubly ionized fragments is also seen.

The infrared spectrum of **1a** shows several readily assignable characteristic features: an N–H stretch at 3356 cm^{-1}, three absorptions around 2900 cm^{-1} due to the methyl group [9], and an absorption at 1356 cm^{-1} which can be assigned as the carboxamido group stretching mode composed of a combination of ν(C–O) and ν(C–N) [9,10].

NMR spectra for **1b** exhibit two inequivalent methyl peaks indicating hindered rotation around the C–N bond (as in an organic amide); this has already been commented upon [4]. The same inequivalence due to restricted rotation around the C–N bond is observed in the spectrum of the N(H)Et complex, **1e**, Fig. 1. In this we see a complex pattern which we analyze as overlapping $ABXY_3/A'B'X'Y_3'$ multiplets. These are separated by 2 Hz as shown by a double resonance experiment in which the signal of the methyl group is saturated; this clearly shows two ABX splitting patterns, separated by 2 Hz. We attribute this result to the existence of two isomers, Et_{axial} and $Et_{equatorial}$, see R_{axial} and $R'_{equatorial}$ in eq. 1 above.

^{1}H NMR spectra of the {μ-O=CNHR} complexes, R = n-Pr or n-Bu, **1c** and **1d** respectively, consist of $ABXY_2$ patterns for the α-methylene protons of each of the carboxamido groups. This could be due either to a smaller chemical shift difference between R_{axial} and R_{radial} isomer, or simply that the steric effect of the bulkier n-propyl and n-butyl groups result in the formation of only one of the two possible isomers; at 200 MHz, a chemical shift difference of less than 2 Hz would be too small to be resolved.

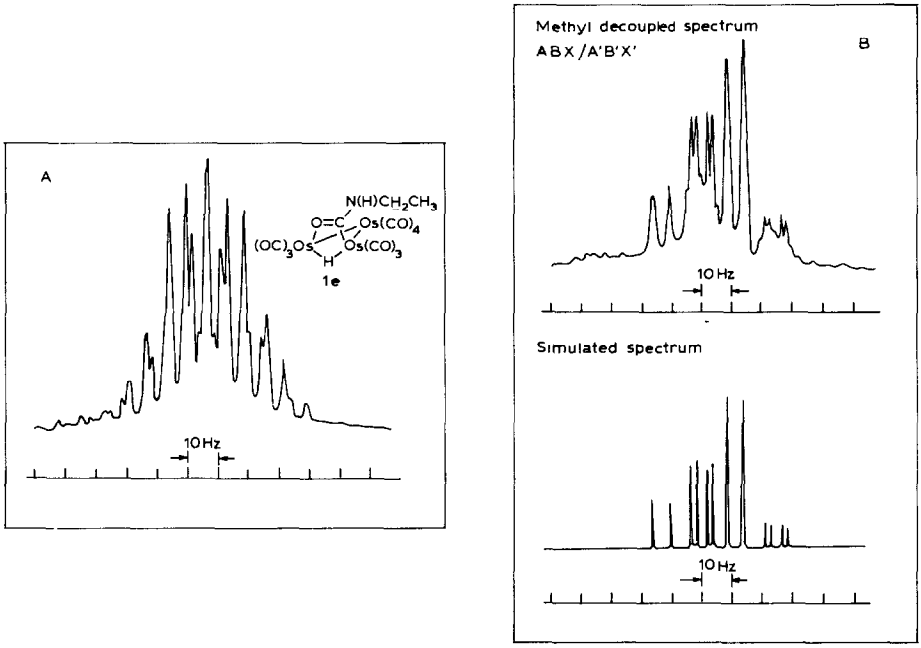

Fig. 1. ^{1}H NMR; 200 MHz, A: methylene signal of the ethyl group in the carboxamido complex $HOs_3(O{=}CN(H)CH_2CH_3)(CO)_{10}$ (**1e**). B. methyl decoupled spectrum together with the simulated ABX/A'B'X' spectrum Bruker 200 WP Spectrometer.

In passing it should be mentioned that some overlap is seen in the $ABXY_3/A'B'X'Y_3'$ pattern for the ethyl complex while the $ABXY_2$ patterns in the n-propyl and n-butyl complexes were clearly separated. This is derived from a much greater value for the ratio $J_{A\text{-}B}/\Delta_{A\text{-}B}$ in the former than in the latter two.

The reaction of $H_2Os_3(CO)_{10}$ with alkyl isocyanates

We were interested to know whether the carboxamido complexes could be prepared by an alternate route. We thus explored the reaction of $Os_3\{\mu\text{-}H\}_2(CO)_{10}$ with methyl isocyanate, see Scheme 1. This yields the μ(O,N)-formamido complex **2a** as a major product.

An *N*-ethyl homolog, **2b**, was also prepared while an *N*-*p*-tolyl homolog, **2c**, and

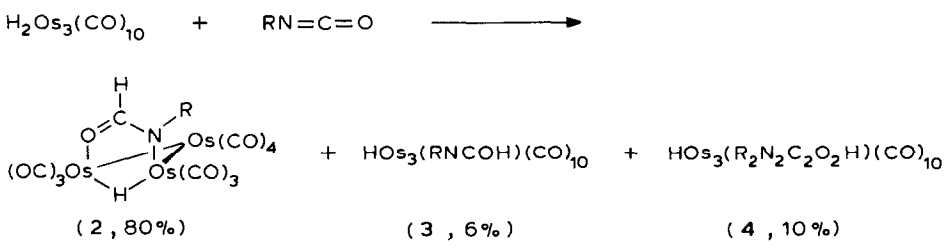

(a, R = Me; b, R = Et)

SCHEME 1

its X-ray structure study was reported by Adams and Golembeski [6] in a parallel and independent study. Spectroscopic data for **2** and other derivatives to be described below are listed in Tables 1 and 2. The IR spectra in the CO stretching region of **2a** and **2b** are essentially the same as that of **2c**. In addition, IR spectra show a peak at 1592 cm^{-1} which can be assigned to the stretching of the O–C=N moiety of the formamido group. The presence of the latter is also indicated by the low field ^1H resonance, δ 7.51 ppm, of the formamido *CH*.

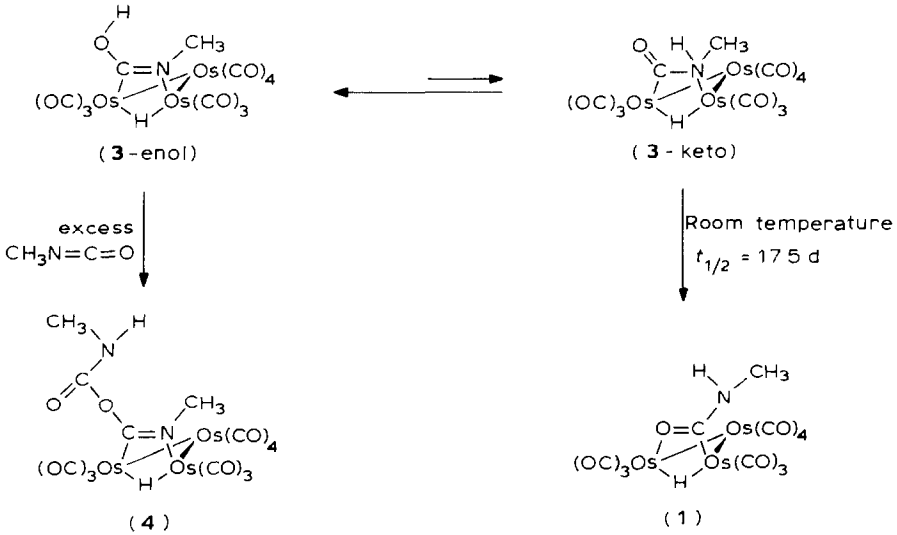

SCHEME 2

The reaction shown in Scheme 1 yields two by-products **3a** and **4a**; though minor, these prove to be highly significant. Complex **3a** is unstable converting to the known $\mu(O,C)$-carboxamido complex **1a** with a half life of 17.5 d at 25 °C in $CDCl_3$ solution, see Scheme 2. Kinetic data for this isomerisation at several different temperatures was obtained; this is discussed further, below.

Spectroscopic data for **3**, and **4** are listed in Tables 1 and 2. Since **3a** is only a minor product in the reaction, attempts were made to improve its yield by changing to solvents of different polarity than that of the neat methyl isocyanate used initially. No dramatic increase of product **3** was observed in tetrahydrofuran, acetonitrile or hexane. We were not able to obtain good single crystals of **3a** for a structure study. Elucidation of its structure depends on the interpretation of its spectroscopic features. This was assisted by knowledge of the structure of **4a** which was determined by X-ray diffraction described in the latter part of this article.

Complex **4** is recognized as a urethane derivative resulting from the reaction of excess methylisocyanate with a hydroxylic precursor. This precursor might well be the enol tautomer of a $\mu(C,N)$-iminyl derivative tentatively assigned as one of two possible isomeric structures for **3**. We return to this point after discussion of the spectral properties of **4a**.

In the infrared spectrum of **4a** [3a or 3c], we see an absorption at 1590 cm^{-1} which is somewhat below 1650 cm^{-1} expected for ν(C=N) [9]. This correlates well

with the bond distance of C=N 1.27 Å (see below) which is just under 1.29 Å for a "standard" carbon to nitrogen double bond [11]. The band at 1770 cm^{-1} is assigned as ν(C=O) of the urethane group and the band at 1590 cm^{-1} as ν(C=N) of the iminyl group. Neither of these change in relative intensity with change in solvent polarity, an important point to contrast with analysis of the spectra of **3**, below. The NMR spectra of the ethyl complex, **4b**, contains two different ethyl peaks; the methylene groups of these are differentiated by different coupling patterns. One of these displays an ABX_3 pattern, where the methylene group possesses two inequivalent protons, ($J_{A\text{-}B}/\Delta_{A\text{-}B} = 0.33$). This is evidently due to the *N*-ethyl iminyl group. The other methylene group displays an AXY_3 pattern and is assigned to the ethyl group in the urethane moiety. The ABX_3 splitting pattern for **3b**, mentioned above, should now be recalled. The similarity in this splitting pattern with that of **4b** provides additional evidence for the enol bonding mode in **3b** ($J_{A\text{-}B}/\Delta_{A\text{-}B} = 0.31$), discussed below.

Returning to **3a**, its mass spectrum shows a peak envelope in the parent multiplet expected for a triosmium carbonyl species. Furthermore, the loss series for ten CO groups is clearly seen as well as that for the doubly ionized species. The mass spectra of the three isomers **1a**, **2a** and **3a** show similar features and are not easily distinguished from each other.

In the infrared spectrum of **3a** [3a or 3c], in C_2Cl_4 solution we see at highest energy the classic absorption of an hydroxyl group, namely a sharp band at 3595 cm^{-1} (free OH) accompanied by a broad band at lower energy centered at 3313 cm^{-1} (hydrogen bonded OH) [9]. An absorption for ν(C–O) is seen at 1225 cm^{-1} and that for (C=N) at 1616 cm^{-1}. A peak is also seen for **3a** at 1795 cm^{-1} which is of diminished relative intensity compared to that observed in hexane. The most likely reason for the change in relative intensity of this peak in solvents of different polarity is the existence of a keto/enol tautomer equilibrium. We assign this peak to ν(C=O) of a keto tautomer of **3a**.

At room temperature of the OH functionality of **3a** is represented by a low field resonance δ 6.56 ppm in the ^1H NMR spectrum. The chemical shift of this resonance is temperature dependent, $\Delta\delta/\Delta T = -1.52$ Hz/K, over the range of 210 to 300 K [3a]. This behavior is typical for organic alcohols [12]. Due to the existence of the keto/enol equilibrium these results might also be due to a fast exchange between the protons of the OH group in the enol tautomer with that of the NH group in the keto tautomer. It is assumed that interconversion between the keto and enol tautomers is fast on the NMR time scale.

*Kinetic study of the isomerization of **3a** to **1a***

The above-mentioned transformation was studied by ^1H NMR. This proved to be the method of choice since all of the absorption peaks due to the two isomers were well separated for measurement of the integrated areas. By contrast, the IR peaks in the CO stretching region of these two isomers are extensively overlapping and do not provide a good means of distinguishing between them let alone following their interconversion.

The transformation of **3a** to **1a** is irreversible. Isomerization however, is not observed if **3a** is kept in the solid state at room temperature. In solution **3a** is not observed to isomerize appreciably over a period of one month below 0 °C. At temperatures above 0 °C, **3a** is slowly isomerized to **1a** in solution. The first

TABLE 3

FIRST ORDER RATE CONSTANT (in min^{-1}) FOR ISOMERIZATION **3a** → **1a** MEASURED BY NMR SPECTRA AT VARIOUS TEMPERATURES

Temperature (K)	Based on NH/OH ratio	Based on Me(d)/Me(s) ratio	Based on metal/hydrogen ratio
333	$(1.60 \pm 0.02) \times 10^{-3}$	$(1.43 \pm 0.02) \times 10^{-3}$	$(1.50 \pm 0.03) \times 10^{-3}$
318	$(3.18 \pm 0.06) \times 10^{-4}$	$(2.81 \pm 0.04) \times 10^{-4}$	$(2.86 \pm 0.05) \times 10^{-4}$
298	$(3.41 \pm 0.06) \times 10^{-5}$	$(2.79 \pm 0.05) \times 10^{-5}$	$(2.91 \pm 0.05) \times 10^{-5}$

temperature at which we could follow isomerization at a measurable rate was at 25 °C. The relative concentrations of **3a** and **1a** were determined by following the areas of three peaks in each isomers [3a]: in **3a**, Os_3H (singlet), CH_3 (singlet) and OH (broad singlet); in **1a**, Os_3H (singlet), CH_3 (doublet) and NH (broad singlet). Rates were measured at three temperatures, 25, 45 and 60 °C. The rate constants fit a first-order law; linear least-squares [13] were applied to calculate a rate constant from each set of data. The rate constants obtained from the ratio of areas of the three characteristic pairs of peaks at each of the three temperatures are listed in Table 3. The temperature dependence of ln(k) is found to be linear [3a]. The slope was calculated by a linear least-squares fit program with equal weight for all data: $E_a = 92 \pm 5$ kJ/mol.

NMR spectra provide confirmation of the existence of the keto tautomer of **3a** for which IR evidence was mentioned above. Peaks attributable to this isomer can only be seen after about half of the **3a** is isomerized to **1a**. The NMR peaks attributed to the keto isomer of **3a** are at δ, ppm: 6.32, NH, 2.94(d) CH_3 and −13.99 for Os-μ-H-Os [3a,3c].

Discussion

Synthesis of $\mu(O,C)$-carboxamido complexes

In the low temperature path under which we have observed formation, in high yield, of the $\mu(O,C)$-carboxamido derivatives we may rule out paths where CO dissociation from $Os_3(CO)_{12}$ is the first step in the reaction. This is based on the known high temperatures which are required for such an unassisted dissociation ($\Delta H^{\neq}$, ca. 30 to 40 kcal/mol) [14]. Instead, we must seek some other explanation for the ease of elimination of CO in the low temperature reaction. In this connection we note that an amine of lower nucleophilicity, namely aniline or amines of greater steric bulk, (trialkyl amines) do not show any interaction with $Os_3(CO)_{12}$ at low temperature.

We propose initial attack by a nucleophile of sufficient strength at the carbon atom of coordinated CO on $Os_3(CO)_{12}$. Deprotonation of the coordinated primary or secondary amine by excess amine would give the anion $[Os_3\{\eta^1\text{-}C(O)NRR'\}(CO)_{11}^-]$. Spectroscopic study of the formation of the carboxamido complexes confirms these postulates: the η^1-carbamoyl complex can be observed by IR (ν(CO) 1650 cm^{-1}) and NMR. In the latter, the methyl groups of the η^1-carbamoyl complex (R = R′ = Me) are observed to be equivalent [3d]. Loss of CO leads to the $\mu(O,C)$-bonded complex in which the ligand shows two different methyl groups.

The loss of a CO group at these exceptionally mild conditions is most likely assisted by the η^1-carbamoyl group (in a position either *geminal, cis* or *vicinal* to the ejected CO). *cis*-Labilization of a carbonyl ligand by the carbamoyl group would be analogous to *cis*-labilization by an acyl group noted by Brown and Bellus for mononuclear complexes [15]. This effect is closely related to the catalysis by nucleophilic bases of substitution reactions in metal hexacarbonyls [16]. Using the "lightly stabilized" [17a] $Os_3(CO)_{11}(CH_3CN)$ [17] as starting material, the reaction is found to be greatly accelerated. The rate of first step (formation of η^1-carbamoyl anion) is thus faster than the second (loss of CO).

By contrast, the high temperature reaction of amines with $Os_3(CO)_{12}$ gives carboxamido complexes in lower yield, mixed with edge-bridged amido complexes, as mentioned in the introduction.

^1H NMR spectroscopic features of the carboxamido complexes

There are three features to note in the ^1H NMR spectra of the carboxamido complexes. The first of these is the characteristic chemical shift of hydrogen as part of the edge double-bridged system. For the $\{\mu\text{-H},\mu(O,C)\}$ isomers, $\delta(\mu\text{-H})$ range from -12 to -14 ppm. For $\{\mu\text{-H},\mu(O,N)\}$ isomers the range for $\delta(\mu\text{-H})$ is -10 to -12 ppm. $\delta(\mu\text{-H})$ for the $\{\mu\text{-H},\mu\text{-RC=NR}'\}$ are grouped slightly higher in energy in the range -14.95 to -15.16 ppm, δ (ppm): -15.02 in $Os_3\{\mu\text{-H},\mu\text{-C(Ph)=N(Me)}\}(CO)_{10}$ [8], -15.15 in $Os_3\{\mu\text{-H},\mu\text{-C(H)=N(Me)}\}(CO)_{10}$, -15.16 in $Os_3\{\mu\text{-H},\mu\text{-C(H)=N(Ph)}\}(CO)_{10}$ and -14.95 in $Os_3\{\mu\text{-H,C(H)=N(Ph)}\}(CO)_9(P(OMe)_3)$ [18].

The two other spectroscopic features of the $\mu(O,C)$-carboxamido group derive on the one hand from the restricted rotation around the C–N bond and on the other hand from chirality induced by its bonding to the cluster. Restricted rotation around the C–N bond gives rise to inequivalent alkyl group resonances, such as the two methyl peaks in the NMR spectrum of the dimethylcarboxamido complex, **1b**. No equilibration can be seen between these resonances up to 120 °C, after which CO is lost from the cluster. By contrast in free amides, equilibration is achieved at 90 °C. In the case of primary amine, an isomer pair is generated, see discussion of Et_{axial} and Et_{radial}, above. The multiple bond character of the C–N bond is seen in the X-ray structure study of the triruthenium analog [2]: the C–N separation is 1.35 Å, intermediate between that expected for a double or for a single bond (1.29 and 1.49 Å respectively, [11]). That the hybridization on the N atom may be best described as sp^2 is also confirmed by the planar geometry around the nitrogen atom [2].

The third spectroscopic feature arises from the chirality of the cluster complex first demonstrated by Deeming and co-workers [19]. All carboxamido complexes containing α-methylene protons in our work show AB patterns in the NMR. A convenient parameter with which to compare these patterns is the ratio $J_{A\text{-}B}/\Delta_{A\text{-}B}$ (where $J_{A\text{-}B}$ is the coupling constant and $\Delta_{A\text{-}B}$ is the difference in the chemical shift of these protons, both in Hz). The constants are listed in Table 4.

While the coupling constants are approximately the same for these complexes, the $\Delta_{A\text{-}B}$ varies from 53.4 Hz to 14.6 Hz. The greater the value of $J_{A\text{-}B}/\Delta_{A\text{-}B}$ the smaller the difference of the AB protons, see for example **2b**. Interestingly for the two ethyl groups in complex **4b**, only the one on the iminyl group is observed to show the AB pattern while the other of the urethane group is represented by an AX_3 signal in the NMR spectrum. Additionally the methylene protons of the *N*-ethyl group in

TABLE 4

^{1}H NMR RESONANCE PARAMETERS OF INEQUIVALENT α-METHYLENE PROTONS IN TRIOSMIUM COMPLEXES

Complex	$J_{A\text{-}B}/\Delta_{A\text{-}B}$	$J_{A\text{-}B}$
1e [a]	0.58	12.26
	0.71	14.23
2b	0.94	13 74
3b	0 31	13 60
4b	0.33	13.60

[a] Two methylene groups due to enantiomers **1e** and **1e′** (see text)

complex **1e** show a closer AB pattern i.e. smaller $\Delta_{A\text{-}B}$ than those in *N*-propyl complex **1c**.

This brings up the question whether the AB pattern is derived from chirality of the cluster or whether it is due either wholly or in part from hindered rotation around the N–CH_2 bond, as mentioned above. To examine this point we first note a temperature dependence in the methylene group resonances of the complex $Os_3\{\mu\text{-}H,\mu\text{-}O{=}C(CH_2C_6H_5)\}(CO)_{10}$ [20]: only a single peak is observed at room temperature while an AB quartet is observed at −130 °C. If the latter is due to chirality of the cluster, its disappearance at room temperature could only be explained by a racemization that is frozen out at lower temperature.

On the other hand, one could also assume insufficient chiral induction from the cluster such that the AB pattern at low temperature comes about from some restriction to rotation around the C–CH_2 bond. Such a restriction arising from *ortho*-metalation is, for instance, seen in the compound $Os_3\{\mu\text{-}H\}_2(\mu\text{-}N(Me)CH_2C_6H_4)\}(CO)_9$ (III) [22], where normally the bridged amido complexes, such as $Os_3\{\mu\text{-}H,\mu\text{-}N(H)n\text{-}Pr\}(CO)_{10}$ (II) show equivalent methylene protons [23].

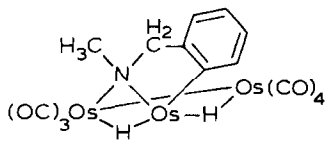

(II)

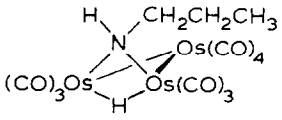

(III)

Of these two possibilities we believe that at least some of the $\Delta_{A\text{-}B}$ observed in the methylene resonances of the μ-O=CN(H)CH_2R groups arise from optical activity on the cluster with some contribution from hindered rotation to explain the variation in $\Delta_{A\text{-}B}$ (see Table 4).

Comments on the formation of various products in the reaction of $Os_3\{H\}_2(CO)_{10}$ with isocyanate

The electronically unsaturated trinuclear osmium complex is known to react with potential σ-donor/π-acceptor ligands to give adducts of the type $HOs_3\{\mu\text{-}H\}(CO)_{10}L$ [24]. It seems reasonable to propose such an adduct for the initial interaction of isocyanate as shown in the middle of Scheme 3.

The reaction next may proceed by addition of Os–H to the various unsaturated centers in the isocyanate in four permutations, A, B, C or D. We have no

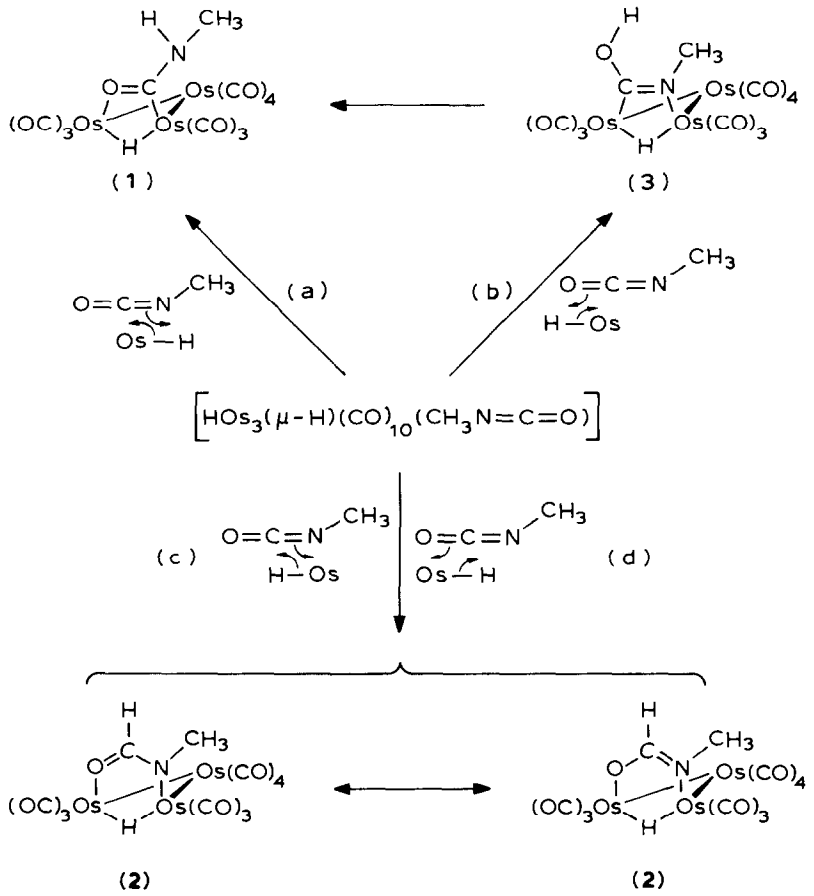

SCHEME 3

information whether such additions are inter- or intra-molecular. Three distinct products are expected, since the two μ(O,N)-isomers, are valence tautomers of each other; these are shown in the lower part of the Scheme. Three products are indeed observed, with the μ(O,N)-isomer as the more prevalent. As discussed elsewhere [3a,b,c], the μ(O,N)-isomer does not interconvert to either the μ(O,C)- or the μ(N,C)-forms. On the other hand, as shown in Scheme 2, we have observed the conversion of the μ(N,C)-isomer to the μ(O,C)-bonded form, repeated in Scheme 3.

For the μ(N,C)-isomer a keto/enol equilibrium was detected with the enol tautomer predominating. The transformation of **3a** to **1a** requires disengagement of the nitrogen from the metal with subsequent coordination of the oxygen. We suggest this isomerization to proceed preferentially in the keto form possessing a quaternary nitrogen atom which would be more easily disengaged as the first step in the transformation. The energy of activation of 92 kJ/mol is a reasonable value for such an Os–N bond breaking process in the transformation.

Spectroscopic identification of all the isomers observed in this work was greatly facilitated by comparison with spectral features of the $\mu(C,N)$-iminylurethane

complex **4a** whose structure we were able to determine. This is described in the latter part of the Experimental Section and the Discussion which follows.

Experimental

General

Solvents and reagents were commercial reagent grade samples which were used without further purification unless otherwise noted. The principal starting material, $Os_3(CO)_{12}$ (**5**) was purchased from Strem Chemicals. $Os_3\{\mu\text{-}H\}_2(CO)_{10}$ (**6**), was prepared according to the literature [25]. Although the products in this work are generally air stable, reactions, filtrations and recrystallizations were routinely carried out under a purified nitrogen atmosphere using Schlenk techniques. Chromatographic separations and handling of neutral complexes can be done in air if exposure is limited to a few hours. Carbonyl infrared spectra were recorded on a Beckman IR-4 spectrometer equipped with LiF optics (calibrated against the cyclohexane peak at 2138.5 cm^{-1}) and a Nicolet MX-1 FT-IR spectrometer. Full range infrared spectra were recorded on a Perkin–Elmer 521 spectrometer and the Nicolet MX-1 FT-IR spectrometer using carbon tetrachloride, deuterochloroform, or tetrachloroethylene as solvents. ^1H and ^{31}P NMR spectra were recorded on a Bruker WP-200 and a JEOL FX90Q spectrometers and calibrated against internal residual $CHCl_3$ at δ 7.25 ppm for proton. Mass spectra were obtained by Dr. K. Fang on an AEI MS-9 spectrometer using a direct inlet probe temperature of 90–120 °C and an ionizating voltage of 70 eV. Elemental analyses were performed by Schwarzkopf Laboratories, Inc.

Syntheses of $Os_3\{\mu\text{-}H,\mu\text{-}O{=}CNR'R\}(CO)_{10}$ (1)

Method A for NRR' = NHMe or NMe_2 and NHEt. A quantity of $Os_3(CO)_{12}$ (**5**, 184 mg, 0.2 mmol) is placed in a 50 ml Schlenk flask equipped with a cold-finger condenser. Under an atmosphere of N_2, the flask is cooled to 0 °C while a dry ice/acetone slurry is placed into the condenser; approximately 2 ml of the amine is condensed into the apparatus directly from either the commercial gas cylinder (H_2NMe, Matheson; $HNMe_2$, Liquid Carbonic) or the 70% aqueous solution of amine (H_2NEt, Baker). The pool of liquid amine at the bottom of the flask dissolves the osmium carbonyl resulting initially in an orange solution which turns yellow over the period of 24 to 36 h. The coolant in the cold finger is allowed to thaw out whereupon the excess amine is evaporated under reduced pressure. The solid residue is dissolved in 1 ml CH_2Cl_2 and then 5 ml hexane is added to facilitate transmittal to a silica gel column (1.9 by 22 cm). A trace of material (less than 3% based on **5**) is first eluted with hexane. The major product is eluted with hexane/CH_2Cl_2, 9/1; yield of **1a** 145 mg (79% based on **5**). The yields of **1b** or **1e** are comparable. A minor product (8 mg, 5%) is eluted with hexane/CH_2Cl_2, 8/2 is observed in the product mix resulting either from the reaction with $MeNH_2$ or Me_2NH. This has not been characterized beyond its ν(CO) (cm^{-1}): 2080m, 2045s, 2023vs, 2001s, 1994w, 1978s, and 1966m. The yield of the minor product depends on the reaction time; for ethyl amine after 10 h, no minor product is observed.

Method B for 1c and 1d. A quantity of **5** (206 mg, 0.23 mmol) is placed into a Schlenk flask under N_2. Amine is added as neat liquid (1.0 ml) (H_2N-n-Pr and H_2N-n-Bu, Aldrich). A solution is formed which first turns orange and then yellow

over a period of 8 to 10 h under stirring. The reaction is worked up as in Method A above; yield of **1c** 180 mg (85% based on **5**). The yield of **1d** is comparable.

*Isolation of $Os_3\{\mu\text{-}H,\mu\text{-}C(OH)=NMe\}(CO)_{10}$ (**3a**) and $Os_3\{\mu\text{-}H,\mu\text{-}C(OR')=NMe\}(CO)_{10}$ (**4a**) R' = C(=O)N(H)Me*

Method A. Neat methyl isocyanate (Aldrich) 0.5 ml, is added to a Schlenk flask containing 176 mg of $Os_3\{\mu\text{-}H\}_2(CO)_{10}$ (**6**, 0.2 mmol) at room temperature under N_2. The purple triosmium cluster quickly dissolves in the isocyanate. The color of the solution fades to yellowish purple in about 15 min. The solution is stirred under nitrogen for another 30 min until it has turned to clear yellow. Excess isocyanate is then removed under reduced pressure. The resulting solid is dissolved into a mixture of hexane/dichloromethane (3 ml/7 ml) and chromatographed on a 1.9 by 22 cm silica gel column. A yellow band quickly elutes with hexane representing a trace amount of an unidentified product (less than 3% by weight of starting material). Another yellow band elutes next which represents **2a** (150 mg, 80% based on **6**). Using hexane/dichloromethane (8/1) a third yellow band is eluted representing **3a** (12 mg, 6% yield). With hexane/CH_2Cl_2 (8/2) a last yellow band elutes representing **4a** (20 mg, 10% yield). Exactly the same procedure is used to prepare the ethyl complexes **2b**, **3b** and **4b** in comparable yields.

Method B. Same reactions have been conducted using hexane, THF, acetonitrile, and iodomethane as solvents. A quantity of **6** is first dissolved in the solvent after which either a two fold excess or a stoichiometric amount of isocyanate was added to the solution. The reactions are monitored by IR. The mixtures are worked up as in method A. Four products are always isolated; yields of **3a** and **4a** vary by $\pm 2\%$.

*Reaction of CH_2N_2 with **3a***

Freshly prepared **3a** (ca. 12 mg) is dissolved in degassed hexane in a Schlenk tube. A solution of CH_2N_2 in ether (5 ml, conc. ca. 0.5 *M*) is slowly added into the tube. After N_2 evolution has ceased the solution is blown dry under a stream of dry nitrogen. Spectroscopic yield of **3a** is quantitative (IR and NMR).

*Isomerization of **3a** to **1a***

Low temperature recrystallization of **3a** is achieved by diffusion of cyclohexane into a chloroform solution. A powdered solid is obtained. This is kept at low temperature if not used immediately. Complex **3a** is dissolved in $CDCl_3$ and sealed under nitrogen into a 5 mm NMR tube. The tube is immersed in an oil bath whose temperature is maintained within 0.5 °C of a designated temperature by a temperature-controller. NMR spectra are periodically monitored until 90% of the **3a** has disappeared. Three peaks attributable to **3a** gradually decrease in intensity while peaks belonging to **1a** appear and gradually increase in relative intensity. Data were recorded at 25, 45, and 60 °C, [3a], and fitted to first order plots.

*Attempted synthesis of a carboxamido complex in the reaction of **6** with dimethylformamide*

N,N-Dimethyl formamide (0.02 ml, 0.26 mmol) is added to a solution of **6** (180 mg, 0.2 mmol) in nonane. No reaction is observed at room temperature even after stirring overnight. The solution is then heated to 150 °C for 3 h. After removal of the nonane and excess of formamide under reduced pressure, the residue is separated by

chromatography on a silica gel column eluting with 10% hexane/dichloromethane. Three bands are obtained: **6** (8 mg, 4%), **1b** (17 mg, 9%), and $Os_4\{\mu\text{-}H\}_4(CO)_{12}$ (35 mg, 17%).

Crystallographic study

Data collection

Suitable crystals of **4a**, $Os_3\{\mu\text{-}H,\mu\text{-}C(OR')=NMe\}(CO)_{10}$, R' = C(=O)N(H)Me *, for X-ray study were grown from hexane solution. Preliminary photographs indicated a monoclinic system. Weissenberg photographs of $(h,0,l)$ and $(h,1,l)$ showed systematic absences for reflections $(h,0,l)$, l odd. In addition, diffractometer data showed absences for reflections $(0,k,0)$, k odd. Space group and cell parameters indicated in Table 5 were uniquely determined.

It was not possible to index the faces of the crystal since this shattered after the data collection. The crystal had been subjected to unusual strain because of an extra cooling and warm-up cycle. The crystal had first been mounted on a Picker four-circle diffractometer and cooled to −158°C before transferring to the Syntex Diffractometer also equipped with a low temperature device [26]; this required warm-up and recooling to −158°C. Approximate dimensions of the crystal were available from the optical centering process. Another crystal of the same morphology was used to index the faces. Six faces bounding the original crystal were determined to be (1,1,0), (1,$\bar{1}$,0), ($\bar{1}$,1,0), ($\bar{1}$,$\bar{1}$,0), (0,0,1) and (0,0,$\bar{1}$) with perpendicular distances from a common point of 0.12, 0.0, 0.07, 0.0, 0.17, 0.0 mm, respectively. The crystal was mounted with the faces $(h,k,0)$ where h and $k = \pm 1$ were roughly parallel to the instrument ϕ axis.

Fifteen strong reflections selected from a polaroid rotation photograph were used as input to the automatic centering, autoindexing and least-squares routines of the diffractometer to obtain a set of low temperature lattice parameters. After data collection, 15 high-angle reflections ($40° < 2\theta < 45°$) were used in the same routine giving a set of accurate cell parameters used for refinement (see Table 5).

Intensity data were collected at −158°C using the $\theta/2\theta$ scan technique with Mo-K_α radiation and a scan rate of 3° min^{-1}. To allow for the presence of both $K_{\alpha 1}$ and $K_{\alpha 2}$ radiation, peaks were scanned from 1.5° in 2θ below the calculated $K_{\alpha 1}$ peak position to 1.5° in 2θ above the calculated $K_{\alpha 2}$ peak position with background counts of one half of the scan time taken at each end of this scan range. The intensities of three standard reflections ($\bar{1}$,1,$\bar{1}$), (1,4,1) and ($\bar{1}$,$\bar{1}$,$\bar{1}$), were measured after every 97 reflections throughout the data collection to monitor crystal and diffractometer stability. The variations in the standards were random; all measurements were within a factor 1.2 of the respective mean values. A total of 3721 independent reflections were measured; this constitutes the entire quarter sphere $+h$, $+k$ and $\pm l$ accessible with Mo-K_α radiation and $0° < 2\theta < 60°$. The 785 reflections having $I < 3\sigma(I)$ were considered to be unobserved and omitted from the

* Following consultations with K.L. Leoning, Nomenclature Director of Chemical Abstracts Service, Columbus, Ohio 43210, the following Chemical Abstracts index name is suggested for **4a**: Decacarbonyl-μ-hydro-μ-(methylcarbamic *N*-methylmethanimidic anhydridato)triosmium(*2-Os–Os*). In line with the IUPAC rules for inorganic chemistry the systematic name is suggested as: Decacarbonyl-μ-hydrido-μ-(methylcarbamic *N*-methylformimidic anhydridato)triosmium (*2-Os–Os*).

TABLE 5

CRYSTAL DATA FOR $HOs_3(\mu\text{-}C(OR)=NCH_3)(CO)_{10}$ (R = C(O)N(H)CH_3)

Crystal system: Monoclinic	V 2099.1(8)Å^3
Space Group: $P2_1/c$	$Z = 4$
a 13.413(2) Å	mol. wt. 966.8 g/mol
b 16.712(3) Å	Density: calc. 3.06 g cm^{-3}
c 9.400(3) Å	obs'd. ----
β 95.011(2)°	Radiation = Mo-$K_{\bar{\alpha}}$, 0.71069 Å
Diffractometer	Syntex $P\bar{1}$
Temperature	−158°C
Scan type	θ–2θ scan at 3.0° min^{-1}
Scan width	$2\theta(K_{\alpha 1})-1.5°$ to $2\theta(K_{\alpha 2})+1.5°$
Reflections measured	$+h, +k, \pm l$; $2\theta = 0°$ to 50°
Reflections collected	3721 (2936 observed)
Absorption coefficient	193.30 cm^{-1}
R^a	0.031
R_w	0.037

[a] $R = \Sigma(||F_o|-|F_c||)/\Sigma|F_o|$; $R_w = [\Sigma w(|F_o|-|F_c|)^2/\Sigma w|F_o|^2]^{1/2}$

refinement. The 2936 observed reflections were corrected for Lorentz and polarization effects and converted to $|F_o|$ and $\sigma(|F_o|)$ by means of the equations:

$$I = SC - \tau(B_1 + B_2)$$

$$\sigma(I) = \left[SC + \tau^2(B_1 + B_2) + p^2I^2\right]^{1/2}$$

$$|F_o| = k\left[I/(Lp)\right]^{1/2}$$

$$\sigma(|F_o|) = (k/2)\left[\sigma(I)\right]/\left[I(Lp)\right]^{1/2}$$

where SC is the count during the scan, τ is the ratio of scan time to background time (= 1 here), B_1 and B_2 are the two background counts, p is the "ignorance factor" (set to 0.04 here), and (Lp) is the Lorentz and polarization factors. Absorption corrections were applied during refinement.

Solution and refinement of structure

Programs used during the structural analysis were locally modified by Dr. C.E. Strouse and his research group. Original programs included the data reduction program PIBAR for the Syntex diffractometer by Bell and Murphy; Fourier programs JBPATT, JBFOUR and PKLIST by Blount; full matrix least-squares and error analysis ORFLS and ORFEE by Busing, Martin and Levy; absorption correction ABSN by Coppens; MGTL by Gantzel and Trueblood for least-squares planes; HPOSN by Hoppe for calculating idealized hydrogen positions; ORTEP by Johnson for the structure plots; and PUBLIST by Hoel for the structure factor table listing. All calculations were performed on the IBM 370/3033 computer (UCLA Office of Academic Computing).

The scattering factors for neutral osmium, oxygen, nitrogen and carbon were taken from Table 2.2A of reference 6a while those for hydrogen were those of Stewart et al. [27]. Both real ($\Delta f'$) and imaginary ($\Delta f''$) components of anomalous dispersion were included for osmium using the values in Table 2.3.1 of ref. 27b.

The function minimized during least-squares refinement was $\Sigma w(|F_o|-|F_c|)^2$

where $w = [\sigma(|F_0|)]^{-2}$. The discrepancy indices are defined as shown in Table 5. The structure was solved by a combination of Patterson and difference Fourier analyses. The positions of the osmium atoms were obtained from a three dimensional Patterson map. Full matrix least-squares refinement on these atoms with isotropic temperature factors produced the residuals $R = 0.133$ and $R_w = 0.189$. A difference Fourier synthesis revealed the positions of all remaining nonhydrogen atoms. Refinement with isotropic temperature factors for all atoms produced the residuals $R = 0.066$ and $R_w = 0.080$. The data were then corrected for the effects of absorption using the assumed indices $(1,\bar{1},0)$, $(\bar{1},1,0)$, $(0,1,0)$, $(0,\bar{1},0)$, $(0,0,1)$, $(0,0,\bar{1})$ for the boundary planes: for μ 193.30 cm^{-1}, max, min and mean transmission factors are 0.552, 0.295 and 0.502, respectively. A cycle of least-squares refinement at this point increased the residuals to $R = 0.093$ and $R_w = 0.105$; this indicated erroneous indexing of the faces.

Another crystal with same morphology was then used to determine the correct indices of all faces. Two cycles of least-squares refinements of positional and isotropic thermal parameters decreased the residuals to $R = 0.041$ and $R_w = 0.049$, indicating the validity of the correction. Three more cycles of least-squares refinement with anomalous dispersion included for osmium and anisotropic thermal parameters for all atoms led to convergence at values of R and R_w as shown in Table 5. The max, min and mean transmission factors obtained in this absorption correction were 0.547, 0.366 and 0.512 respectively.

At this point, a difference Fourier map indicated the position of some methyl hydrogen atoms, but the hydrogen atom bridging the edge of the cluster could not be clearly located. Attempts to find this atom using maps derived only from the low angle reflections [28] ($\sin\theta < 0.333$) was also unsuccessful. Location of the bridging hydrogen was finally achieved through a difference map after the two methyl groups were refined as idealized rigid groups. We first assumed C–H bond distances of 1.00 Å and tetrahedral CH_3 group and calculated initial hydrogen atom positions for the two methyl groups using chemically reasonable hydrogen positions observed in the previous difference map. The bridging hydrogen was then located, bridging between atoms Os(2) and Os(3); its positional parameters were refined with the isotropic thermal parameter arbitrarily assigned as 4.0 Å.

Positional and thermal parameters of the bridging and N–H hydrogen atoms were not included in the last refinement. The final atomic positions are given in Table 6. Tables of thermal parameters, root-mean-square amplitudes of vibration and structure factors are available in ref. [3a] or from NAPS *.

Description of the structure and discussion

Overall structure. The crystal consists of discrete molecular units of $Os_3\{\mu\text{-H},\mu\text{-C(OR)=NCH}_3\}(CO)_{10}$ where $R = C(=O)N(H)CH_3$. The geometry of the molecule and the system used for labeling atoms are illustrated in Fig. 2. Interatomic distances and presented in Table 7 and interatomic angles in Table 8.

The triangular cluster of osmium atoms contains Os–Os separations in the range 2.881(1) to 2.924(1) Å (see Table 8). A selection of related triosmium cluster

* Materials have been deposited with the National Auxiliary Publications Service, c/o Microfiche Publications, P.O.; Box 3513, Grand Central Station, New York, N.Y. 10017, U S.A.

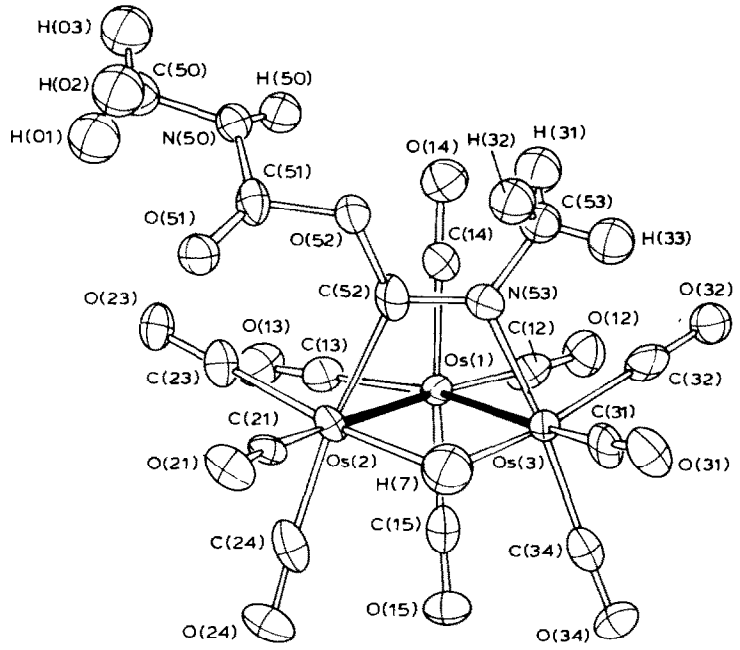

Fig. 2. ORTEP projection of $HOs_3(\mu\text{-}C(OR)=NMe)(CO)_{10}$, R = C(O)N(H)Me; thermal ellipsoid at 50% probability.

compounds for comparison of Os–Os separations is offered in Table 9 *, containing some derivatives mentioned above as well as new ones introduced in references [29] through [38]. For comparison, the Os–Os separations in $Os_3(CO)_{12}$ are listed in a footnote to Table 9. A more comprehensive list may be seen in reference [39]. Of particular relevance to this study are the bridged metal–metal distances in complexes containing 2 atom bridges accompanying the bridging hydrogen. These are seen to be consistently longer, on the order of 0.05 Å, than those of the nonbridged metal–metal separations.

One edge of the triangular cluster is doubly bridged, first by hydrogen atom located 0.43(12) Å out of the trimetal plane and also by a *C*-methylcarbamic *N*-methyl iminyl group also out of the trimetal plane but on the side opposite to the bridging hydrogen atom. The imino group is attached to the cluster through its C and N atoms located at disctances of 1.92(1) and 1.91(1) Å, respectively, from the metal plane.

The geometry about each osmium atom is approximately octahedral. The carbonyl groups which help to define this are discussed separately below. We intentionally

* To compare Os–Os separations due note must be taken of bond order. The Os–Os separation in $Os_3(\mu\text{-}H)_2(CO)_{10}$ is shortened relative to its unbridged edges (and relative to $Os_3(CO)_{12}$) because the order of the bond between osmium atoms at the doubly bridged edge is 2 [7,29]. In other complexes listed where the edge bridged by hydrogen is also bridged by a three-electron donating group, the bond order between the osmium atoms is taken to be one. Comparisons within this group are thus in order.

TABLE 6

FINAL ATOMIC POSITIONS[a,b] OF $HOs_3(\mu\text{-}C(OR)=NCH_3)(CO)_{10}$(R = C(O)N(H)$CH_3$)

Atom	x	y	z
Os(1)	0.25419(3)	−0.01735(3)	0.39846(5)
Os(2)	0.29200(3)	0.03810(3)	0.11785(5)
Os(3)	0.09941(3)	0.06903(3)	0.23091(5)
C(12)	0.2026(9)	−0.0405(7)	0 578(1)
O(12)	0.1764(6)	−0 0537(5)	0 6877(9)
C(13)	0.3839(9)	−0 0652(7)	0 437(1)
O(13)	0.4600(7)	−0 0957(5)	0 4632(9)
C(14)	0.3004(9)	0.0875(7)	0.467(1)
O(14)	0.3269(6)	0.1484(5)	0 5102(8)
C(15)	0.1937(9)	−0 1135(7)	0.311(1)
O(15)	0.1576(7)	−0.1725(5)	0.2680(9)
C(21)	0.3078(9)	0.0768(6)	−0.073(1)
O(21)	0.3179(7)	0.0959(5)	−0.1854(8)
C(23)	0.4327(9)	0 0301(7)	0 170(1)
O(23)	0.5161(6)	0.0253(5)	0 2018(9)
C(24)	0.2844(9)	−0.0720(7)	0.050(1)
O(24)	0.2786(7)	−0 1351(5)	0 0041(9)
C(31)	0.0045(9)	0.1315(7)	0 114(2)
O(31)	−0.0560(7)	0.1704(6)	0 0529(9)
C(32)	0.0493(9)	0.0932(7)	0.410(1)
O(32)	0.0182(7)	0.1102(5)	0.5142(9)
C(34)	0.0181(9)	−0.0249(7)	0 206(1)
O(34)	−0.0353(6)	−0 0775(5)	0.1859(8)
N(50)	0.5046(7)	0 2335(6)	0 274(1)
C(51)	0.4399(8)	0.2115(6)	0 167(1)
O(51)	0.4569(6)	0.1929(5)	0.0466(8)
C(52)	0.2787(9)	0.1566(7)	0.196(1)
O(52)	0.3430(6)	0.2194(4)	0.2093(8)
N(53)	0.1928(7)	0.1716(5)	0.2382(9)
C(50)	0.6119	0.2316	0.2575
H(01)	0.6394	0.1782	0.2330
H(02)	0.6082	0.2669	0.1712
H(03)	0.6567	0.2566	0.3357
C(53)	0 1663	0.2508	0.2916
H(31)	0.2035	0.2587	0 3874
H(32)	0.1885	0.2918	0.2236
H(33)	0.0929	0.2566	0.3000
H(50)	0.4743	0.2330	0.3376
H(7)	0.1504	0 0623	0.0697

[a] Positions are given in fractional coordinates. [b] The estimated standard deviation of the least significant digit is given in parentheses. This is based on the final least squares correlation matrix including contributions due to errors in the unit cell parameters.

leave out the vector between Os(2) and Os(3) in the ORTEP projection, see Footnote p. 208.

Bridging hydrogen and the metal–metal separations. The bridging hydrogen in the present molecule was located with reasonable precision and these positional parameters were well behaved during the least-squares refinement procedure, while its isotropic thermal parameter was kept at 4.0 Å^2. The Os(2)–H–Os(3) bridge is

TABLE 7

INTERATOMIC DISTANCES (Å) [a] FOR $HOs_3(\mu\text{-}C(OR)=NCH_3)(CO)_{10}$ (R = C(O)N(H)CH_3)

Os(1)–Os(2)	2.8823(9)	Os(2)–Os(3)	2.9240(9)
Os(1)–Os(3)	2.8816(8)	Os(2)–C(52)	2.13(1)
Os(1)–C(12)	1.91(1)	Os(2)–C(21)	1.93(1)
Os(1)–C(13)	1.92(1)	Os(2)–C(23)	1.91(1)
Os(1)–C(14)	1.95(1)	Os(2)–C(24)	1.95(1)
Os(1)–C(15)	1.95(1)	Os(2)–H(7)	1.96(12)
Os(1)–O(12)	3.057(8)	Os(2)–O(21)	3.058(8)
Os(1)–O(13)	3.067(8)	Os(2)–O(23)	3.047(9)
Os(1)–O(14)	3.090(8)	Os(2)–O(24)	3.086(8)
Os(1)–O(15)	3.103(8)		
C(12)–O(12)	1.14(1)	C(21)–O(21)	1.13(1)
C(13)–O(13)	1.15(1)	C(23)–O(23)	1.13(1)
C(14)–O(14)	1.14(1)	C(24)–O(24)	1.14(1)
C(15)–O(15)	1.16(1)		
Os(3)–N(53)	2.122(9)	C(52)–N(53)	1.27(1)
Os(3)–H(7)	1.72(12)	C(52)–O(52)	1.36(1)
Os(3)–C(31)	1.92(1)	O(52)–C(51)	1.40(1)
Os(3)–C(32)	1.91(1)	C(51)–N(50)	1.33(1)
Os(3)–C(34)	1.91(1)	C(51)–O(51)	1.21(1)
Os(3)–O(31)	3.067(9)	N(50)–C(50)	1.46
Os(3)–O(32)	3.043(8)	N(53)–C(53)	1.47
Os(3)–O(34)	3.050(8)	C(32)–O(32)	1.13(1)
C(31)–O(31)	1.15(1)	C(34)–O(34)	1.14(1)

[a] See footnote *b*, Table 6.

found to be unsymmetrical: Os(2)–H 1.96(12) and Os(3)–H 1.72(12) Å. Previous studies [40] give r(H) as 0.3 Å. Taking r(Os) as 1.44 Å from the nonbridged osmium–osmium separations in the present molecule, a terminal Os–H distance is thus expected to be 1.74 Å. This average of the two Os–H distances found in this molecule of 1.84 Å, is somewhat longer, owing perhaps to the bridge-bonding mode. This is in agreement with the separations observed in several other hydrogen bridged osmium cluster complexes as also summarized in Table 9. In these, the Os–H separation in the bridged systems is seen to vary anywhere from 1.72 to 2.03 Å.

The bridged Os(2)–Os(3) distance is lengthened by only 0.04 Å relative to the nonbridged Os–Os distances. This is a result of two opposing effects [30]. A bridging hydrogen atom unaccompanied by any other groups bridging on the same edge is seen generally to increase metal separations on the order of 0.10 to 0.13 Å; however, an accompanying bridging ligand such as an imino group, produces constraints to oppose this lengthening.

The μ-iminyl group. This is seen as a nearly symmetrical bridge across the Os(2)–Os(3) bond: Os(3)–N(53) 2.122(9) Å, while Os(2)–C(52) 2.13(1) Å. The imino-carbon–nitrogen distance C(52)–N(53) 1.27(1) Å, is close to that expected for a carbon to nitrogen double bond (C–N, 1.49; C=N, 1.29; C≡N, 1.15 Å) [11], and is similar to the distance 1.28(1) Å observed for this bond in $Os\{\mu\text{-}H,\mu\text{-}C(C_6H_5)=N(CH_3)\}(CO)_{10}$ [8b]. The carbon-nitrogen distances for η^1-imino groups in some mononuclear complexes are, by way of comparison (Å): 1.27(1) in $(\eta^5\text{-}C_5H_5)Mo(CO)_2(P(OCH_3)_3)(\eta^1\text{-}C(CH_3)=N(C_6H_5)$, [41] and 1.29 in $Pt(P(C_6H_5)_3)_2(\eta^1\text{-}C(CH_3)=N(C_6H_4Cl))$ [42]. A dihapto-iminyl group, on the other

TABLE 8

BOND ANGLES (degrees) FOR $HOs_3(\mu\text{-}C(OR)=NCH_3)(CO)_{10}$ (R = C(O)N(H)CH_3) [a]

Os(2)–Os(1)–Os(3)	60.97(2)	Os(1)–Os(2)–Os(3)	59.51(2)
Os(2)–Os(1)–C(12)	167.3(3)	Os(1)–Os(2)–H(7)	91.9(*)
Os(2)–Os(1)–C(13)	94.5(4)	Os(1)–Os(2)–C(52)	87.5(3)
Os(2)–Os(1)–C(14)	86.4(3)	Os(1)–Os(2)–C(21)	176.1(3)
Os(2)–Os(1)–C(15)	88.9(3)	Os(1)–Os(2)–C(23)	89.5(3)
Os(3)–Os(1)–C(12)	106.5(3)	Os(1)–Os(2)–C(24)	89.4(3)
Os(3)–Os(1)–C(13)	155.5(4)	Os(3)–Os(2)–H(7)	34.6(*)
Os(3)–Os(1)–C(14)	85.6(3)	Os(3)–Os(2)–C(52)	66.8(3)
Os(3)–Os(1)–C(15)	86.0(3)	Os(3)–Os(2)–C(21)	116.7(3)
C(12)–Os(1)–C(13)	98.0(5)	Os(3)–Os(2)–C(23)	143.3(4)
C(12)–Os(1)–C(14)	91.1(5)	Os(3)–Os(2)–C(24)	105.3(4)
C(12)–Os(1)–C(15)	91.9(5)	C(52)–Os(2)–H(7)	77.2(*)
C(13)–Os(1)–C(14)	93.2(5)	C(52)–Os(2)–C(21)	91.7(4)
C(13)–Os(1)–C(15)	94.2(5)	C(52)–Os(2)–C(23)	95.0(5)
C(14)–Os(1)–C(15)	171.5(4)	C(52)–Os(2)–C(24)	172.0(5)
Os(1)–C(12)–O(12)	177(1)	C(21)–Os(2)–H(7)	84.2(*)
Os(1)–C(13)–O(13)	178(1)	C(21)–Os(2)–C(23)	94.4(5)
Os(1)–C(14)–O(14)	178(1)	C(21)–Os(2)–C(24)	91.0(4)
Os(1)–C(15)–O(15)	176(1)	C(23)–Os(2)–H(7)	172.0(*)
		C(23)–Os(2)–C(24)	92.3(5)
		Os(2)–C(21)–O(21)	177(1)
Os(1)–Os(3)–Os(2)	59.52(3)	Os(2)–C(23)–O(23)	180(1)
Os(1)–Os(3)–H(7)	97.2(*)	Os(2)–C(24)–O(24)	177(1)
Os(1)–Os(3)–N(53)	89.5(2)		
Os(1)–Os(3)–C(31)	175.6(4)		
Os(1)–Os(3)–C(32)	85.2(4)	Os(2)–C(52)–N(53)	113(2)
Os(1)–Os(3)–C(34)	91.9(3)	Os(2)–C(52)–O(52)	132.2(1.4)
Os(2)–Os(3)–H(7)	40.2(*)	N(53)–C(52)–O(52)	114.7(1.9)
Os(2)–Os(3)–N(53)	67.4(3)		
Os(2)–Os(3)–C(31)	116.9(3)	Os(3)–N(53)–C(52)	112.2(8)
Os(2)–Os(3)–C(32)	138.4(3)		
Os(2)–Os(3)–C(34)	108.8(3)	C(52)–N(53)–C(53)	122
N(53)–Os(3)–H(7)	78.6(*)		
N(53)–Os(3)–C(31)	86.5(4)	O(51)–C(51)–O(52)	123(1)
N(53)–Os(3)–C(32)	93.1(4)	O(51)–C(51)–N(50)	128(1)
N(53)–Os(3)–C(34)	174.5(4)	O(52)–C(51)–N(50)	108(1)
C(31)–Os(3)–H(7)	80.0(*)		
C(31)–Os(3)–C(32)	97.1(5)	C(52)–O(52)–C(51)	119.9(8)
C(3)–Os(3)–C(34)	91.9(5)		
C(32)–Os(3)–H(7)	171.2(*)	C(51)–N(50)–C(50)	120
C(32)–Os(3)–C(34)	92.4(5)	C(51)–N(50)–H(50)	104(1)
C(34)–Os(3)–H(7)	95.9(*)	C(50)–N(50)–H(50)	134

[a] See Footnote *b*, Table 6.

hand, shows significant bond-shortening: C–N 1.233(6) Å in $(\eta^5\text{-}C_5H_5)Mo(CO)_2(\eta^2\text{-}C(CH_3)=N(C_6H_5)$ [41].

The urethane group bonded to the cluster through the iminyl carbon atom in the present complex is seen with the expected structural features. The C(51)–N(50) distance lies between that of a single and a double bond (see above), indicating delocalization as expected in this group.

Carbonyl groups. The mutually *trans*-axial carbonyl ligands on the $Os(CO)_4$

TABLE 9

METAL–METAL SEPARATIONS FOR TRIOSMIUM CARBONYL CLUSTER COMPLEXES CONTAINING A BRIDGING GROUP ACCOMPANYING BRIDGING HYDROGEN

Compound	Os–Os separation (Å)			Os–H (Å)	Ref.
	Unbridged [b]	Bridged	Diff.		
$Os_3(\mu\text{-}H)_2(CO)_{10}$	2.817(1), 2.812(1)	1.681(1)	−0.132	1.845(3)	29
$Os_3H(\mu\text{-}H)(CO)_{11}$	2.910(1), 2.857(1)	2.989(1)	+0.106	[a]	30
$Os_3H(\mu\text{-}H)(CO)_{10}(PPh_3)$	2.917(1), 2.865(1)	3.019(1)	+0.128	1.74(6) 2.00(6) 1.52(7) (t)	24c
One-atom bridge accompanying μ-H					
$Os_3(\mu\text{-}H)(\mu\text{-}Cl)(CO)_{10}$	2.829(1), 2.836(1)	2.846(1)	+0.013	[a]	31
$Os_3(\mu\text{-}H)(\mu\text{-}Br)(CO)_{10}$	2.844(1), 2.842(1)	2.851(1)	+0.008	2.03(14) 2.03(14)	32
	2.838(1), 2.834(1)	2.876(1)	+0.040	[a]	
$Os_3(\mu\text{-}H)(\mu\text{-}OMe)(CO)_{10}$	2.813(1), 2.822(1)	2.812(1)	−0.006	1.93(11) 1.84(11)	33
$Os_3(\mu\text{-}H)(\mu\text{-}SEt)(CO)_{10}$	2.842(2), 2.856(2)	2.863(2)	+0.014	[a]	34
$(HOs_3(CO)_{10})_2(SCH_2S)$	2.872(1), 2.854(1)	2.867(1)	−0.004	[a]	35
	2.875(1), 2.875(1)	2.871(1)	+0.004	[a]	
$Os_3(\mu\text{-}H)(\mu\text{-}N(H)SO_2C_6H_4Me)(CO)_{10}$	2.858(1), 2.847(1)	2.814(1)	−0.039	1.91(8) 1.96(8)	36
$Os_3(\mu\text{-}H)(\mu\text{-}C(H)CH{=}NEt_2)(CO)_{10}$	2.866(2), 2.870(2)	2.785(2)	−0.083	1.76(15) 1.82(17)	37
$Os_3(\mu\text{-}H)(\mu\text{-}C(H)CH)_2PMe_2Ph)(CO)_{10}$	2.873(1), 2.869(1)	2.800(1)	−0.071	1.95(7) 1.80(8)	38
Two-atom bridge accompanying μ-H					
$Os_3(\mu\text{-}H)(\mu\text{-}PhC{=}NMe)(CO)_{10}$	2.863(1), 2.892(1)	2.918(1)	−0.041	[a]	8b
$Os_3(\mu\text{-}H)(\mu\text{-}HC{=}NPh)(CO)_9(P(OME)_3)$	2.863(1), 2.893(1)	2.961(1)	+0.083	[a]	18
$Os_3(\mu\text{-}H)(\mu\text{-}ROC{=}NMe)(CO)_{10}$, (R=C(=O)N(H)Me)	2.882(1), 2.882(1)	2.924(1)	+0.042	1.72(12) 1.96(12)	[c]
$Os_3(\mu\text{-}H)(\mu\text{-}O{=}CNHC_6H_4Me)(CO)_9(P(Me)_2Ph)$	2.859(1), 2.893(1)	2.945(1)	−0.069	[a]	6b
Three-atom bridge accompanying μ-H					
$Os_3(\mu\text{-}H)(\mu\text{-}OCHNC_6H_4Me)(CO)_{10}$	2.888(1), 2.903(1)	2.909(1)	+0.014	[a]	6b
$Os_3(\mu\text{-}H)(\mu\text{-}OCHNC_6H_4Me)(CO)_9(P(Me)_2Ph)$	2.897(1), 2.911(1)	2.940(1)	+0.036	[a]	6b

[a] M–H distances are not determined. [b] By way of comparison the Os–Os distances in $Os_3(CO)_{12}$ are (Å): 2.882, 2.875, 2.874 (ave. 2.877) [30]. [c] This work.

group along with carbonyl ligand trans to the imino C-atom on Os(2) have the longest Os–C distances (Os(1)–C(14) 1.95(1), Os(1)–C(15) 1.95(1), and Os(2)–C(24) 1.95(1) Å). The former two can readily be explained by competition for back-donated

π-electron density for mutually *trans*-π-acceptor ligands. This is also reflected in the osmium–oxygen distances which are correspondingly the longest in Os(1)–O(14) 3.090(8) and Os(1)–O(15) 3.103(8) Å. The fact that Os(2)–C(24) also is long may indicate that a strong bond exists between Os(2) and the imino atom C(52). By comparison, the separation Os(3)–C(34) 1.91(1) Å, is the shortest Os–C(carbonyl) observed in this molecule. Thus the imino C atom seems to be a better π-acceptor than the imino N atom. These results are also observed in $Os_3\{\mu\text{-}H,\mu\text{-}C(C_6H_5)=N(CH_3)\}(CO)$ [8b].

Acknowledgment

This work was supported by a grant from the National Science Foundation (CHE-79-08406) and a NATO fellowship from the DAAD (German Academic Exchange Service) to A.M.. Computing costs were supported in part by an intramural grant from the UCLA Academic Computing Center.

References and notes

1 (a) M.A. Andrews and H D. Kaesz, J. Am. Chem. Soc., 101 (1979) 7238 and 7255; (b) M.A Andrews, G. Van Buskirk, C.B. Knobler and H.D. Kaesz, ibid., 101 (1979) 7245; (c) M.A. Andrews, C.B. Knobler and H.D. Kaesz, ibid., 101 (1979) 7260.
2 R. Szostak, C.E. Strouse and H.D. Kaesz, J. Organomet. Chem., 191 (1980) 243.
3 (a) Y C. Lin, Dissertation, UCLA, 1981; (b) Y.C. Lin, C.B. Knobler and H.D. Kaesz, J. Am. Chem. Soc., 103 (1981) 1216; (c) H.D Kaesz, C.B. Knobler, M.A. Andrews, G. Van Buskirk, R Szostak, C.E. Strouse, Y.C. Lin, and A. Mayr, Pure & Appl. Chem., 54 (1982) 131; (d) A. Mayr, Y.C. Lin, N.M Boag and H.D. Kaesz, Inorg. Chem., 21 (1982) 1704.
4 K.A. Azam, C.C. Yin and A.J. Deeming, J. Chem. Soc. Dalton, (1978) 1201
5 (a) M. Tachikawa, Ph.D Thesis, Univ. of Illinois, Urbana-Champaign, 1977; (b) B.F.G. Johnson, J. Lewis, T.I. Odiaka and P.R. Raithby, J. Organomet. Chem., 216 (1981) C56.
6 (a) R.D. Adams and N.M. Golembeski, J. Organomet. Chem., 171 (1979) C21; (b) R.D. Adams, N.M. Golembeski and J.P. Selegue, Inorg. Chem., 20 (1981) 1242.
7 (a) R. Mason and D.W.P. Mingos, J. Organomet. Chem., 50 (1973), 53; (b) B.K. Teo, M.B. Hall, R.F Fenske, and L.F. Dahl, ibid., 70 (1974) 413; (c) N.M. Kostic and R.F. Fenske, Inorg. Chem., 22 (1983) 666.
8 (a) C.C. Yin and A.J. Deeming, J. Organomet. Chem., 133 (1977) 123; (b) R.D. Adams and N.M. Golembeski, Inorg. Chem., 17 (1978), 1969.
9 L.J. Bellamy, Advances in Infrared Group Frequencies, Chapman and Hall, London, 1975.
10 R. Szostak, Dissertation, UCLA, 1981
11 Special Pub. Chem. Soc. (London), 1968, Nos. 15&18.
12 A.L. Van Geet, Anal. Chem., 42 (1970), 679.
13 P.R. Bevington, Data Reduction and Error Analysis for the Physical Scientists, McGraw-Hill Inc., New York, NY, 1969.
14 F. Basolo and R.G. Pearson, Mechanisms of Inorganic Reactions, John Wiley and Sons, New York, 1967.
15 (a) T.L. Brown and P.A. Bellus, Inorg. Chem., 17 (1978) 3726; (b) idem, J. Am. Chem. Soc., 102 (1980) 6020.
16 (a) D.E. Morris and F. Basolo, J. Am. Chem. Soc., 90 (1968) 2536; (b) R.J. Angelici, Acct. Chem. Res., 5 (1972) 335.
17 (a) M. Tachikawa and J.R. Shapley, J. Organomet. Chem., 124 (1977) C19; (b) B.F.G. Johnson, J Lewis and D. Pippard, ibid., 145 (1978) C4; (c) B.F.G. Johnson, J. Lewis and D. Pippard, J. Chem. Soc. Dalton, (1981) 407.
18 R.D. Adams and N.M. Golembeski, J Am. Chem. Soc., 101 (1979) 2579.
19 A.J. Arce and A.J. Deeming, J. Chem. Soc. Chem. Comm., (1980) 1102
20 K.A. Azam, A.J. Deeming and P. Rothwell, J. Chem. Soc. Dalton, (1981) 91.

21 A.D. Clauss, M. Tachikawa, J.R. Shapley and C.G. Pierpont, Inorg. Chem., 20 (1981) 1528.
22 R.D. Adams and J.P. Selegue, Inorg. Chem., 19 (1980) 1791.
23 E.G. Bryan, B.F.G. Johnson and J. Lewis, J. Chem. Soc. Dalton, (1977) 328.
24 (a) A.J. Deeming and S. Hasso, J. Organomet. Chem., 114 (1976), 313; (b) J.R. Shapley, J.B. Keister, M.R. Churchill and B.G. DeBoer, J. Am. Chem. Soc., 97 (1975) 4145; (c) M.R. Churchill and B.G. DeBoer, Inorg. Chem., 16 (1977) 2397.
25 S.A.R. Knox, J.W. Koepke, M.A. Andrews and H.D. Kaesz, J. Am. Chem. Soc., 97 (1975) 3942.
26 C.E. Strouse, Rev. Sci. Instrum., 47 (1976) 871.
27 (a) International Tables for X-ray Crystallography, Vol. IV, Kynoch Press, Birmingham, England 1975; (b) R.F. Stewart, E.R. Davidson and W.T. Simpson, J. Chem. Phys., 42 (1965) 3175.
28 (a) S.J. la Placa and J.A. Ibers, J. Am. Chem. Soc., 85 (1963), 3501; (b) idem. Acta. Cryst., 18 (1965) 511.
29 (a) M.R. Churchill, F.J. Hollander and J.P. Hutchinson, Inorg. Chem., 16 (1977) 2697; (b) R.W. Broach and J.M. Williams, Inorg. Chem., 18 (1979) 314.
30 M.R. Churchill and B.G. DeBoer, Inorg. Chem., 16 (1977) 878.
31 M.R. Churchill and R.A. Lashewycz, Inorg. Chem., 18 (1979) 3261.
32 M.R. Churchill and R.A. Lashewycz, Inorg. Chem., 18 (1979) 1926.
33 M.R. Churchill and H.J. Wasserman, Inorg. Chem., 19 (1980) 2391.
34 V.F. Allen, R. Mason and P.B. Hitchcock, J. Organomet. Chem., 140 (1977) 297.
35 R.D. Adams and N.M. Golembeski, J. Am. Chem. Soc., 101 (1979) 1306.
36 M.R. Churchill, F.J. Hollander, J.R. Shapley and J.B. Keister, Inorg. Chem., 19 (1980) 1272.
37 M.R. Churchill and R.A. Lashewycz, Inorg. Chem., 18 (1979) 848.
38 M.R. Churchill and B.G. DeBoer, Inorg. Chem., 16 (1977) 1141.
39 M.I. Bruce in G. Wilkinson, F.G.A. Stone, and E.W. Abel, (Eds.), Comprehensive Organometallic Chemistry: Index of Structures Determined by Diffractions Methods; Pergamon Press, New York, 1982, Vol. 9, p. 1446–1447.
40 (a) R.G. Teller and R. Bau, Structure and Bonding, 44 (1981) 1; (b) L. Pauling, The Nature of the Chemical Bond, Cornell University Press, Ithaca, N.Y. 1960: Table 7-4, p. 226.
41 (a) R.D. Adams and D.P. Chodosh, J. Organomet. Chem., 122 (1976) C11; (b) idem., Inorg. Chem., 17 (1978) 41.
42 K.P. Wagner, P.M. Treichel and J.C. Calabrese, J. Organomet. Chem., 71 (1974), 299.